Check for updates

Phosphorus availability from olivine for biospheres

Josh Abbatiello[1], John E. Henson[1] and Matthew Pasek[1,2]*

[1]School of Geoscience, University of South Florida, Tampa, FL, United States, [2]Department of Earth and Environmental Sciences, Rensselaer Polytechnic Institute, Troy, NY, United States

Phosphorus plays a multifaceted role for all known life and hence understanding its sources on the early Earth provides constraints on how life developed to incorporate this element into its biochemistry. Currently, the major phosphorus mineral group on the surface of the Earth are the apatites, which are poorly soluble calcium phosphates and hence may not have been a good source of phosphorus on the early Earth. An alternative source of phosphorus may be the mineral olivine. Given that olivine makes up a large part of the upper mantle of Earth and presumably other rocky planets and moons, it stands to reason that olivine may be a potential phosphorus reservoir for prebiotic chemical environments. Here we examine the phosphorus content of 10 olivine samples from different terrestrial localities to determine their P content and P speciation. We find that extracts of the samples contain varying amounts of phosphate, and some contain pyrophosphate. Olivine may have served as a source of phosphate on the early Earth and possibly elsewhere in the solar system, and its dissolution could have supplied this nutrient to a nascent biosphere.

KEYWORDS

phosphorus, astrobiology, habitability, olivine, dissolution

1 Introduction

Phosphorus is an element central to many aspects of modern biochemistry. The phosphate moiety is important to several classes of biomolecules such as phospholipids that make up cell membranes, metabolic molecules such as adenosine triphosphate (ATP), and as part of the backbone of DNA (with deoxyribose) allowing for its polymeric structure. In contrast to the other biogenically critical elements [carbon, hydrogen, oxygen, nitrogen, and sulfur (C, H, O, N, and S or CHONS)], phosphorus does not possess a significant volatile phase and does not participate in redox reactions over a large range of conditions commonly present on the Earth's surface. In life, organisms extract phosphorus from mineral sources or remove it from water or recycle it from existing biomolecules. However, this presents a major hurdle for understanding how biologically important phosphorus molecules developed prior to the formation of life on rocky planets. The apatite mineral group [including hydroxyapatite ($Ca_5(PO_4)_3OH$) and fluorapatite ($Ca_5(PO_4)_3F$)] is considered to have been the source of phosphate on the surface of the early Earth and likely elsewhere, but the apatite mineral group is by and large unreactive and insoluble in water, which may have prevented phosphorus from being bioavailable on a large scale (Gulick, 1955). Given the importance of phosphorus to the development of terrestrial life, phosphorus's abundance and its availability may serve as important indicator of the habitability of a planet or moon, such as Mars (Adcock et al., 2013) and Enceladus (Hao et al., 2022; Postberg et al., 2023).
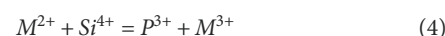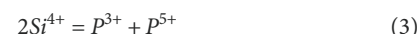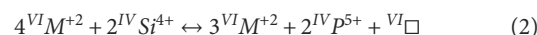
If apatite was the primary source of phosphate on the early Earth this leads to what is known as the "phosphate problem" in the origin of life community (Fernández-García et al., 2017). Apatite's poor solubility and low reactivity make it a rather difficult material from which to make the key organics of life (Pasek, 2008). Typical concentrations of phosphate in the environment are on the order of 10^{-6} M and below (Tyrrell, 1999) whereas many phosphorylation experiments use levels much higher than that, on the order of 0.1–1 M (Xu et al., 2019; Cheng et al., 2002; Reimann and Zubay, 1999). However, some environments may provide elevated phosphate. Recently, Last Chance Lake and Goodenough Lake in Canada were demonstrated to contain up to 37 mM of phosphate, the highest natural levels recorded thus far (Haas et al., 2024), though the source of this phosphate still ultimately was mineral dissolution during weathering. Other hypotheses have been put forth to describe how the environment may have afforded an increased phosphate reactivity including alternative solvents that are not pure water to promote dehydration, using condensing agents to promote water loss, heating phosphates with organic compounds, and the possibility that reduced phosphorus sources that oxidize to produce reactive phosphates (Lago, 2021; Schoffstall, 1976; Pasek et al., 2007; Lohrmann and Orgel, 1968).

In addition to the apatite group, the mineral olivine ((Mg,Fe)$_2$SiO$_4$) also bears phosphorus, and may have been a major source of phosphate on the early Earth by virtue of its ubiquity (Walton et al., 2021a). Olivine is a mineral that is a primary component of the Earth's upper mantle and is the first to crystallize out of magma. Olivine is also common to many meteorites (Bridges and Warren, 2006). Olivine has two compositional end members, forsterite (Mg$_2$SiO$_4$) and fayalite (Fe$_2$SiO$_4$), and natural occurrences are generally a solid solution of these two, usually with more forsterite (Fo) than fayalite (Fa) in the ultramafic rock peridotite (Elias and Alderton, 2020). Peridotite is a major component of the Earth's upper mantle believed to be formed by partial melting of the mantle with the rising molten portion of mantle (Elias and Alderton, 2020). Olivine is initially more forsteritic when it crystallizes out of magma, potentially allowing for phosphorus incorporation due to lattice mismatching (see below) (Welsch et al., 2013). Recently, olivine has been shown to incorporate phosphorus at a higher rate than previously thought due to a number of factors (Agrell et al., 1962; Bekker et al., 2021; Boesenberg and Hewins, 2010; Li et al., 2017; Lynn et al., 2017; McKibbin et al., 2019; Shea et al., 2019; Shea et al., 2015; Walton, 2022; Welsch et al., 2014; Walton et al., 2021b).

Phosphoran olivine is a variety of olivine that bears a P$_2$O$_5$ content greater than 1 weight %. Most olivine is not phosphoran, and has a largely variable phosphorus content ranging from a lower end of 0.07–0.15 weight % (Brunet and Chazot, 2001) to an upper range of 0.3–0.6 weight % (Welsch et al., 2013). Under normal olivine crystal growth rate, phosphorus is an incompatible element in the olivine lattice, meaning due to the ionic radius and valence of phosphorus it will preferentially partition into the melt (Lynn et al., 2020). Phosphorus will slowly diffuse into the olivine crystal and only in these very small amounts (Baziotis et al., 2017). During rapid formation (growth rate of 10^{-6} m/s) of an olivine crystal, branch misorientations and lattice mismatching may occur potentially allowing for a higher percentage of phosphorus incorporation into the crystal structure (Welsch et al., 2014). Due to a similarity in

atomic size, phosphorus (P^{5+}) likely replaces silicon (Si^{4+}) in the structure of olivine during this rapid growth (Welsch et al., 2013). Further, a less-stiff crystal lattice during rapid growth may be the explanation for phosphorus incorporation (Shea et al., 2019). The composition of the melt and the crystallization process of olivine seem to be the main controls on the incorporation of phosphorus into the olivine lattice (Ersoy et al., 2019).

The generally accepted substitution mechanism for most olivine is phosphorus (P^{5+}) replaces silicon (Si^{4+}) in the tetrahedral site (Equation 1) (Milman-Barris et al., 2008). However, Boesenberg and Hewins (2010) demonstrated a vacancy (denoted "□") in the octahedral site with phosphorus substitution correlated to a cation deficiency (Equation 2) in phosphoran olivine. They also concluded that phosphoran olivine is metastable and forms from a phosphorus rich melt, with the maximum amount of P$_2$O$_5$ being around 27 weight %. Phosphorus substitution in the octahedral site could also be from the phosphite (P^{3+}) ion balancing out the deficit of charge if P$_2$O$_5$ (P^{5+}) and P$_2$O$_3$ (P^{3+}) were both present in the olivine grain (Equation 3). Fourthly, aluminum is a common ion found zoned in olivine displaying similar patterns to phosphorus [(Welsch et al., 2013; Shea et al., 2019; Baziotis et al., 2017; Ersoy et al., 2019; Milman-Barris et al., 2008)]. Milman-Barris et al. (2008) examined olivine that exhibited increasing aluminum and chromium (both 3+ cations) content as phosphorus increased. It is plausible that some of the charge balancing occurring is phosphite (also 3+) substitution into the olivine structure (Equation 4).

$$5Si^{4+} = 4P^{5+} + □ \tag{1}$$

$$4^{VI}M^{+2} + 2^{IV}Si^{4+} \leftrightarrow 3^{VI}M^{+2} + 2^{IV}P^{5+} + {}^{VI}□ \tag{2}$$

$$2Si^{4+} = P^{3+} + P^{5+} \tag{3}$$

$$M^{2+} + Si^{4+} = P^{3+} + M^{3+} \tag{4}$$

To this end, we investigated 10 olivine samples from around the world to check for the presence of alternative P redox states (e.g., Equations 3, 4), and to better constrain the amount of P released from olivine during extraction with a chelating agent. These data may then better constrain the role of extremely abundant olivine as a source of P on the early Earth and on other rocky planets.

2 Methods

The ten olivine sample localities are provided in Table 1, along with the median composition (in terms of Fo%, or percentage Mg vs. Mg + Fe). Samples were examined by XRD to verify they were only olivine (Feng et al., 2024). Between 0.5 and 0.6 g of olivine crystals were crushed to a fine powder using a mortar and pestle, placed in glass vials with 1.5 mL of sodium ethylenediaminetetraacetic acid (Na$_4$EDTA) (Sigma Aldrich) which was brought up to a pH of 13 using sodium hydroxide (Alfa Aesar) and placed onto a magnetic stir plate for 1 week. After extraction, the liquid was filtered using 0.22 μm filter tips (Biomed Scientific) fixed to a 1 mL syringe and placed on watch glasses to dry for 2 days. Once dried, 500 μL of D$_2$O (Sigma Aldrich) was added

TABLE 1 Locations of olivine samples analyzed and corresponding forsterite range.

Location	County or sublocation	Composition
North Carolina, United States of America	Jackson County	Fo$_{80-94}$ (Feiss et al., 1991)
New Jersey, United States of America	Gloucester County	Fo$_{57-70}$ (Gorring and Naslund, 1995)
Hawaii, United States of America	Papakōlea beach	Fo$_{80-90}$ (Garcia, 1996)
Norway	Vanylven municipality	Fo$_{92-93}$ (Osland, 1997)
Pakistan	Sapat Gali (Kohistan)	Fo$_{78-92}$ (Jan et al., 1993)
Spain	Almeria Province	Fo$_{89-92}$ (Trommsdorff et al., 1998)
New Mexico, United States of America	Taos	Fo$_{49-83}$ (Aoki, 1967)
Mexico	Popocatépetl	Fo$_{88-90}$ (Roberge et al., 2007)
Arizona, United States of America	San Carlos	Fo$_{90-91}$ (Abramson et al., 1997)
Italy	Terragnolo	Fo$_{87-88}$ (Renna and Tribuzio, 2011)

to each watch glass, mixed, and using a pipet the solutions were placed into Eppendorf tubes for centrifugation to separate the solution from any remaining solid. The supernatants were placed in Wilmad Nuclear Magnetic Resonance (NMR) tubes (Sigma Aldrich) and were analyzed via Bruker Neo 600 MHz NMR running for 6,000 scans, for H-decoupled ^{31}P NMR (242.8609732 MHz) at the University of South Florida (USF) Interdisciplinary NMR Facility. All spectra were analyzed using Mnova version 14.3.3 package.

100 mg of phosphonoacetic acid (C$_2$H$_5$O$_5$P) (98%, Sigma Aldrich) was added into 1 mL of Milli-Q 18 mOhm deionized water purified in house using a Barnstead (Dubuque, IA) Nanopure Diamond Analytical combined reverse osmosis-deionization system. This resulted in a phosphonoacetic acid solution of 0.7 M. 20 μL of the phosphonoacetic acid solution was added to each NMR tube and analyzed at the same USF NMR facility.

The analysis for total P was performed on a Perkin-Elmer Nexion 2000 Quadrupole Inductively Coupled Plasma–Mass Spectrometer (ICP-MS). The same EDTA process was employed again to prepare the samples. 400 μL was diluted to 10 mL using the same deionized water. In between each sample analysis a blank of deionized water with a solution of 15% ethanol (C$_2$H$_6$O) was ran through all parts of the system followed by a 5% solution of trace metal grade nitric acid (HNO$_3$). The solutions were used to clean the lines and the internal components of the ICP to prevent build-up of organic residue. A calibration curve was made using a solution of P (High Purity Standards, 1,000 ppm with serial dilutions to 1 ppm). A blank of EDTA was also measured to ensure no cross contamination was occurring from that source. The measurement of the EDTA measured at less than 10 ppb. A nine-point calibration curve was used to create a linear equation which was then manually applied to each sample after analysis was complete. The relative standard deviation (RSD) of the samples averaged out to be less than 3% throughout the entire run.

3 Results

The phosphorus speciation of 10 olivine samples was examined using ^{31}P NMR (Figure 1). Phosphate of varying quantities was detected in each of the 10 samples. Pyrophosphate was clearly detected in the samples from Hawaii and Pakistan.

Three methods were employed to determine the total phosphate concentration extracted for each sample (Table 2; Figure 2). In the first method, a known concentration and quantity of phosphonoacetic acid was added to each olivine extract. The samples were then run, and spectra analyzed by taking the integrations of phosphonoacetic acid and phosphate peak. The mass of P extracted was then determined using the integrated ratio and amount of initial olivine sample. In the second method, the phosphate NMR "signal" was compared at its highest intensity to three times the standard deviation of the "noise" ranges. The signal value was divided by the average noise and squared to obtain a concentration as per Pasek et al. (2007). These methods were contrasted to the concentration determined by ICP-MS.

4 Discussion

The mineral apatite is usually considered to be the *de facto* source of prebiotic phosphorus by prebiotic geochemists as it comprises 80% of the modern phosphorus reservoir, and apatite is soluble in mantle melts and common in the continental crustal (Walton et al., 2021a). The potential of olivine to be a major source of phosphorus on the early Earth has received comparatively little consideration (Walton et al., 2021a).

Pasek et al. (2022), in a study of serpentinites and phosphorus, hypothesized that in the presence of iron (II), the reduction of phosphate to phosphite could occur in the olivine itself, and that serpentinization merely releases this phosphorus as phosphite. In this study, we find no evidence of phosphite in 10 terrestrial olivine samples from different localities, suggesting that P in olivine is
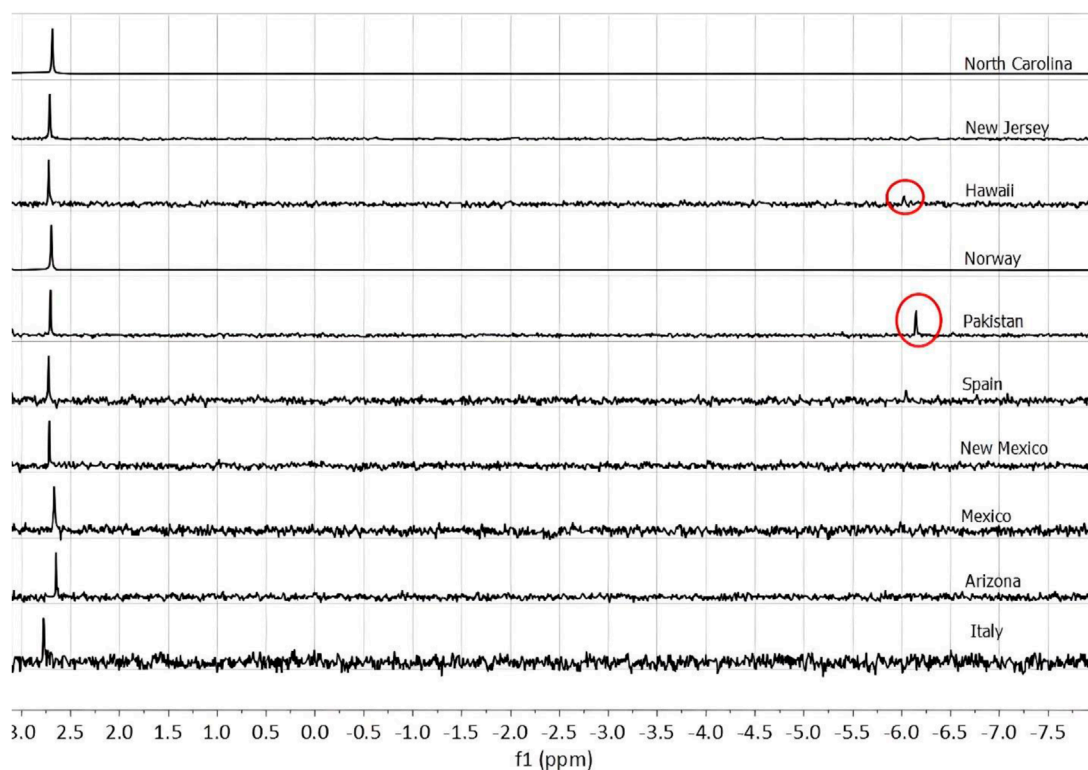
FIGURE 1
NMR spectra showing phosphate (PO_4^{3-}) peaks at roughly 2.7 ppm. The Hawaiian and Pakistani olivine samples show pyrophosphate ($P_2O_4^{7-}$) peaks in circles. The samples from Spain and new Jersey may also have a peak corresponding to pyrophosphate.

TABLE 2 Phosphorus content extracted and relative quantities of phosphate (Pi) and pyrophosphate (PPi).

Location	P (ppm)	Pi: (%)	PPi
North Carolina, United States of America	149	100	ND
New Jersey, United States of America	4.8	100	ND
Hawaii, United States of America	34.4	63	37%
Norway	21	100	ND
Pakistan	6.3	65	35%
Spain	8.3	100	ND
New Mexico, United States of America	3.5	100	ND
Mexico	5.3	100	ND
Arizona, United States of America	3.3	100	ND
Italy	3.2	100	ND

present only as P^{5+}. Therefore, the serpentinization process likely leads to phosphate reduction to phosphite.

Pyrophosphate was in olivine samples from Hawaii and Pakistan, and possibly in the samples from Spain and New Jersey.

Phosphate has been shown at high temperatures ($\sim$1,000 K) in the presence of silicate glass to be polymerized into pyrophosphate at a large percentage (Mysen, 1996). At such temperatures, the phosphate begins to exchange oxygens with the silicate species, resulting in a more polymerized phosphorus and less polymerized silicate (Mysen, 2011). The relative quantity of phosphate to pyrophosphate (as measured through peak integration) in the Hawaiian olivine is 63% phosphate and 37% pyrophosphate and 65% phosphate and 35% pyrophosphate in the Pakistani olivine, suggesting some polymerization of phosphate to pyrophosphate during crystallization, or perhaps some other process is effecting this change. Given the absence of pyrophosphate in most samples, the formation of pyrophosphate may be a mineralogic or petrologic process, as opposed to being an artifact of our sample preparation procedure. Notably pyrophosphate may have been relevant to the development of life on the earth, based on the presence of pyrophosphatase enzymes (Baltscheffsky et al., 1966), where pyrophosphate serves as an energy molecule akin to ATP. However, some of these enzymes are not widespread across all domains of life (Segami et al., 2018) hence natural pyrophosphate may have had a mixed effect on early biosystems: it may have been useful as a biologic energy molecule but may have also not been easy for early organisms to use as a P source.

The presence of phosphorus in olivine provides a broader context for other planets. For example, Chassingnite meteorites from Mars (as part of the SNC Martian meteorites) are
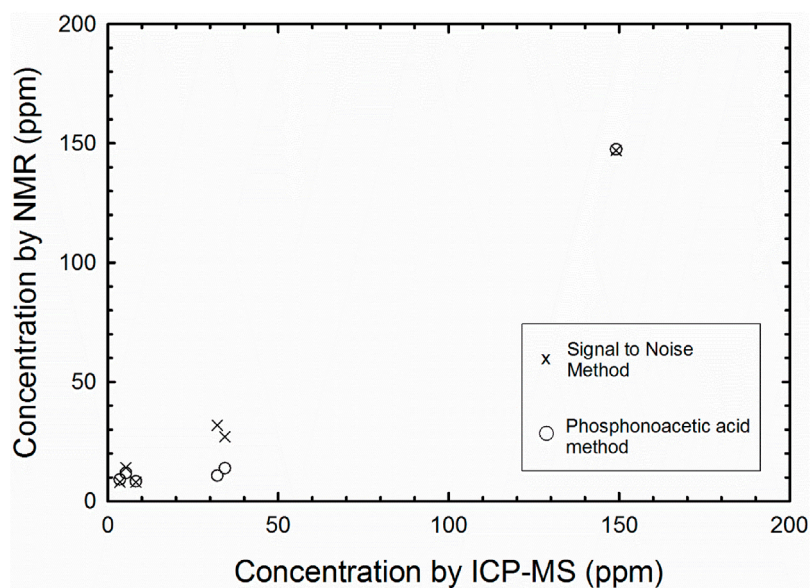
FIGURE 2
Scatter plot showing trend of NMR signal to noise ratio ("x") compared to samples spiked with phosphonoacetic acid (circles), both compared to results from ICPMS.

dunites [composed of ~90% olivine (Mason, 1981)]. The Chassigny meteorite has 0.018 wt% P within it (Banin et al., 1992; Maciá et al., 1997). It is plausible that dunites on Mars could have served as P sources, given their possible wide-spread occurrence. Olivine located on the Martian surface have been postulated as indicative of primitive mantle magmas (McSween et al., 2006) and various olivine cumulate outcrops have been identified, in some cases composing up to 65% of the rock material present (Liu et al., 2022; Mustard et al., 2005; Hamilton and Christensen, 2005).

For these reasons, olivine could have been a source of phosphorus on Mars to a nascent, early biosphere. Although extractions of Mars dunites like the extractions performed above are too costly given the scarcity of this material, we would also anticipate Mars olivine to be a source of pyrophosphate, though at a lower scale than of phosphate.

Europa and Enceladus are both of particular interest when exploring the potential of olivine as a source of phosphorus on other worlds where life may have developed. Due to the subsurface oceans likely present on both moons (Carr et al., 1998; Pappalardo et al., 1999; Roberts and Nimmo, 2008; Thomas et al., 2016), water-rock interactions between olivine and the ocean may have liberated phosphate into water. Olivine present in the mantle boundary interacting with the ocean could lead to the release of phosphorus from the olivine as phosphate, as well as through the process of serpentinization (Pasek et al., 2022). The crust and mantles of both Europa and Enceladus have been theorized to be composed of olivine similar to that of Earth's mantle (Schubert et al., 2009; Hsu et al., 2015). Hao et al. (2022) argued for the efficient release of phosphate by binding of divalent cations with carbonate from CO_2 and by enhancing dissolution with lower pH (Hao et al., 2022). Evidence for higher phosphate at Saturn's moon Enceladus is

further supported by analyses by the Cassini Cosmic Dust Analyzer, which suggested that sodium phosphates were a component of some of the icy particles of Saturn's e-ring (Postberg et al., 2023), the source of which appears to be Enceladus. This suggests the subsurface water at Enceladus may bear more phosphate than previously envisioned (Carr et al., 1998), with olivine as a potential source.

In comparison to the measured P contents of olivine (Welsch et al., 2013; Agrell et al., 1962; Bekker et al., 2021; Boesenberg and Hewins, 2010; Li et al., 2017; Lynn et al., 2017; Brunet and Chazot, 2001; Baziotis et al., 2017; Ersoy et al., 2019; Buseck and Clark, 1984), the average phosphorus content we extracted was between 3 and 150 ppm. The EDTA extraction method has been shown to work with other samples to establish phosphorus speciation including soils (Bowman and Moir, 1993; Turner et al., 2003), fulgurites (Pasek and Block, 2009), and serpentinites (Pasek et al., 2022). The amount of P extracted by this method is typically 50–90+% (Turner et al., 2003). We chose to use a soil science P extraction procedure given these prior successes, and the fact that the EDTA solution does not appear to alter phosphorus speciation. In contrast, a more aggressive extraction procedure (using a strong acid such as HCl or HF) would likely have caused the hydrolysis of P species including pyrophosphate and possibly caused oxidation of any reduced P compounds. That said, the relatively low extraction using this method contrasts with these prior measurements and suggests that the phases extracted with EDTA are likely easier to extract when linked to chelatable ions (such as Ca and Fe). The phosphate in these samples is likely bound to Mg and substitutes for Si. For this reason, we posit that the likelihood of olivine serving as a P-supplying material on the early Earth and other planets is instead limited to the dissolution of olivine.

4.1 Olivine as a model phosphorus-supplying material

We investigate two scenarios to constrain the release of P from olivine dissolution in the environment. The first scenario (Equation 5) considers the low release from a global, perfectly spherical shell/crust of olivine dissolving in a global ocean. The second (Equation 6) considers a localized region where small olivine grains dissolve to release P, modeled after the green sand Papokolea Beach, Hawaii. Note that each of these cases explores the initial, linear dissolution of olivine (which is usually given in length over time). As dissolution proceeds, the rate of dissolution slows due to increasing concentrations of ions, among other factors (Hausrath and Brantley, 2010). As such, they represent maxima and will likely decrease to a steady-state system where P is released at the same rate it is removed (for instance, by crystallization of phosphates or through adsorption).

In the minimal scenario, we consider the release of P from olivine within the whole Earth's crust, assuming the crust is a sphere.

$$P_{Earth} = \left(SA_{Earth} \times k_{Oli} \right) \times \%oli_{Up} \times \%P_{oli} \qquad (5)$$

In this calculation SA_{Earth} is the surface area of the Earth or 5.1×10^8 km^2, k_{Oli} is the dissolution rate of olivine in water or 7×10^{-14} mol/cm^2/s at 298K and 1 atm of pressure (Pokrovsky and Schott, 2000), $\%oli_{Up}$ is the percentage of olivine in the upper mantle or 55% (Langmuir and Broecker, 2012), and $\%P_{oli}$ is the percentage range of phosphorus estimated to be in terrestrial olivine samples or 0.07–0.6 weight % (Bekker et al., 2021; Brunet and Chazot, 2001). From these data, the total potential phosphorus released globally through the dissolution of olivine ranged from $6 \times 10^8 - 5.7 \times 10^9$ kg/year. This corresponds to a molarity of $2.1 \times 10^{-13} - 4.2 \times 10^{-12}$ phosphorus present in the ocean released each year.

In the olivine sand beach environment, the P released can be much higher locally. We determine this through:

$$P_{Beach} = \left(SA_{TotGrains} \times k_{Oli} \right) \times \%P_{oli} \qquad (6)$$

where $SA_{TotGrains}$ is the estimated surface area of the total grains of olivine sand on Papokolea Beach or 7.7×10^{13} m^2 (see SI), k_{Oli} is the dissolution rate of olivine in water or 7×10^{-14} mol/cm^2/s, and $\%P_{oli}$ is the percentage range of phosphorus estimated to be in terrestrial olivine samples or 0.07–0.6 weight %. From these data, the total potential phosphorus released locally through the dissolution of olivine ranged from $2 \times 10^2 - 2 \times 10^3$ kg P/year. This corresponds to a molarity of 0.5 to 4 M phosphorus present in the estimated water surrounding the beach, which would certainly be supersaturated with respect to phosphate mineral precipitation. This number hence represents an ideal case without precipitation, and it is much more likely that the concentration of phosphate would be limited by the decreasing dissolution of olivine and onset of precipitation of other minerals, such as serpentinite minerals. Fuhr et al. (2022) present data arguing a maximum olivine dissolution of ~1 mM, at which point other minerals begin to precipitate (Fuhr et al., 2022). Note that in both this case (Equation 6) and the minimal calculation (Equation 5), dissolution would compete with reaction of olivine with water to form serpentinite minerals. Which process would dominate would be a function of local pressure, temperature, and other conditions (Olsen et al., 2015).

$$P_{Apatite} = \left(\%_{ApCrust} \times M_{Crust} \times \%_{Phos} \right) \times K_{apatite} \qquad (7)$$

We compare these olivine dissolution values to the potential phosphorus released via apatite on a global scale using Equation 7 where M_{Crust} is 1.40×10^{20} kg (Walton et al., 2021a), $\%_{ApCrust}$ is the percentage of the crust being composed of apatite (Jahnke, 1992), $\%_{Phos}$ is the percentage of phosphate in the bulk Earth (crust) or 0.15%, and $K_{apatite}$ is the dissolution rate of apatite in water or 8.16×10^{-10}-3×10^{-7} mol m^{-2} s^{-1} (Adcock et al., 2013). From these data, the total potential phosphorus released globally through the dissolution of apatite ranges from 1×10^8 and 5×10^{10} kgP/year. This range fits well with previously modeled ocean apatite values (1.4×10^9 kg/yr^{-1} and 4.2×10^{10} kg/yr (Jusino-Maldonado et al., 2022; Paytan and McLaughlin, 2007). This corresponds to a molarity range of $1.19 \times 10^{-13} - 3.98 \times 10^{-11}$ of phosphorus present in the ocean.

It is apparent from these models that olivine dissolution may exceed phosphate release from the dissolution of apatite, especially in localized environments. It is unclear though what occurs following this release. The phosphorus could immediately crystallize into apatite, via reaction with Ca^{2+}. It is possible that the phosphorus may react with iron and reduce to phosphite (Herschy et al., 2018). It may also adsorb onto silica gel and create microenvironments for production of prebiotically relevant molecules (Westall et al., 2018). Nonetheless, the release of phosphate from olivine dissolution may have provided an additional source of bioavailable phosphate, through the slow dissolution of abundant olivine.

5 Conclusion

Phosphorus as phosphate was present in all 10 terrestrial olivine samples from different localities. Phosphorus was mainly present as phosphate, but some amounts of pyrophosphate were in at least two samples. The phosphate in the samples ranged from 3.2–149 ppm released during these extractions. Pyrophosphate was the only other P species observed released from olivine. The potential for olivine to be a viable source of phosphorus on the early Earth seems promising. The range of phosphorus in olivine on a global scale is equal to and in some cases greater than that of apatite. This holds true on a local environment scale as well such as the one modeled for Papokolea beach, Hawaii. Although olivine beaches are uncommon today, they may have been more prevalent on an early Earth where island arc accretion would have helped form the early crustal rocks [e.g. (Korsch et al., 2011)].

Data availability statement

The original contributions presented in the study are included in the article/Supplementary Material, further inquiries can be directed to the corresponding author.

Author contributions

JA: Data curation, Investigation, Methodology, Resources, Validation, Visualization, Writing–original

draft, Writing–review and editing. JH: Methodology, Writing–review and editing. MP: Conceptualization, Funding acquisition, Investigation, Methodology, Project administration, Resources, Supervision, Writing–original draft, Writing–review and editing.

Funding

Conflict of interest

The authors declare that the research was conducted in the absence of any commercial or financial relationships that could be construed as a potential conflict of interest.

Publisher's note

Supplementary material

The Supplementary Material for this article can be found online at: https://www.frontiersin.org/articles/10.3389/fspas.2024.1441187/full#supplementary-material

References

Abramson, E., Brown, J., Slutsky, L., and Zaug, J. (1997). The elastic constants of San Carlos olivine to 17 GPa. *J. Geophys. Res. Solid Earth* 102 (B6), 12253–12263. doi:10.1029/97jb00682

Adcock, C., Hausrath, E., and Forster, P. (2013). Readily available phosphate from minerals in early aqueous environments on Mars. *Nat. Geosci.* 6 (10), 824–827. doi:10.1038/ngeo1923

Agrell, S., Charnley, N., and Chinner, G. (1962). *Phosphoran olivine from pine canyon*, 2. Utah Miner: Piute Co, 265–269.

Aoki, K.-i. (1967). Petrography and petrochemistry of latest Pliocene olivine-tholeiites of Taos area, northern New Mexico, USA. *Contributions Mineralogy Petrology* 14 (3), 190–203. doi:10.1007/bf00376639

Baltscheffsky, H., von Stedingk, L.-V., Heldt, H.-W., and Klingenberg, M. (1966). Inorganic pyrophosphate: formation in bacterial photophosphorylation. *Science* 153 (3740), 1120–1122. doi:10.1126/science.153.3740.1120

Banin, A., Clark, B., and Wänke, H. (1992). "Surface chemistry and mineralogy," in Mars, Los. Angel, January 1, 1992, (United States: University of Arizona Press), 594–625. doi:10.2307/j.ctt207g59v.22

Baziotis, I., Asimow, P., Ntaflos, T., Boyce, J., McCubbin, F., Koroneos, A., et al. (2017). Phosphorus zoning as a recorder of crystal growth kinetics: application to second-generation olivine in mantle xenoliths from the Cima Volcanic Field. *Contributions Mineralogy Petrology* 172, 58–32. doi:10.1007/s00410-017-1376-7

Bekker, T., Litasov, K., Shatskiy, A., Sagatov, N., Podborodnikov, I., and Krinitsin, P. (2021). Experimental and *ab initio* investigation of the formation of phosphoran olivine. *ACS Earth Space Chem.* 5 (6), 1373–1383. doi:10.1021/acsearthspacechem.1c00011

Boesenberg, J. S., and Hewins, R. H. (2010). An experimental investigation into the metastable formation of phosphoran olivine and pyroxene. *Geochimica Cosmochimica Acta* 74 (6), 1923–1941. doi:10.1016/j.gca.2009.12.008

Bowman, R., and Moir, J. (1993). Basic EDTA as an extractant for soil organic phosphorus. *Soil Sci. Soc. Am. J.* 57 (6), 1516–1518. doi:10.2136/sssaj1993.03615995005700060020x

Bridges, J., and Warren, P. (2006). The SNC meteorites: basaltic igneous processes on Mars. *J. Geol. Soc.* 163 (2), 229–251. doi:10.1144/0016-764904-501

Brunet, F., and Chazot, G. (2001). Partitioning of phosphorus between olivine, clinopyroxene and silicate glass in a spinel lherzolite xenolith from Yemen. *Chem. Geol.* 176 (1-4), 51–72. doi:10.1016/s0009-2541(00)00351-x

Buseck, P. R., and Clark, J. (1984). Zaisho—a pallasite containing pyroxene and phosphoran olivine. *Mineral. Mag.* 48 (347), 229–235. doi:10.1180/minmag.1984.048.347.06

Carr, M. H., Belton, M. J., Chapman, C. R., Davies, M. E., Geissler, P., Greenberg, R., et al. (1998). Evidence for a subsurface ocean on Europa. *Nature* 391 (6665), 363–365. doi:10.1038/34857

Cheng, C., Fan, C., Wan, R., Tong, C., Miao, Z., Chen, J., et al. (2002). Phosphorylation of adenosine with trimetaphosphate under simulated prebiotic conditions. *Orig. Life Evol. Biosphere* 32, 219–224. doi:10.1023/a:1016513114799

Elias, S., and Alderton, D. (2020). *Encyclopedia of geology*. Academic Press.

Ersoy, Ö., Nikogosian, I. K., van Bergen, M. J., and Mason, P. R. (2019). Phosphorous incorporation in olivine crystallized from potassium-rich magmas. *Geochimica Cosmochimica Acta* 253, 63–83. doi:10.1016/j.gca.2019.03.012

Feiss, P. G., Maybin, I. I. I. A. H., Riggs, S. R., and Grosz, A. E. (1991). *Mineral Resources of the carolinas*. Knoxville TN: The Geology of the Carolinas: Carolina Geological Society Fiftieth Anniversary, 319.

Feng, T., Omran, A., Gull, M., Schaible, M. J., Orlando, T. M., and Pasek, M. A. (2024). Schreibersite oxidation under varied oxygen buffers. *Geochimica Cosmochimica Acta* 380, 140–148. doi:10.1016/j.gca.2024.07.022

Fernández-García, C., Coggins, A. J., and Powner, M. W. (2017). A chemist's perspective on the role of phosphorus at the origins of life. *Life* 7 (3), 31. doi:10.3390/life7030031

Fuhr, M., Geilert, S., Schmidt, M., Liebetrau, V., Vogt, C., Ledwig, B., et al. (2022). Kinetics of olivine weathering in seawater: an experimental study. *Front. Clim.* 4, 39. doi:10.3389/fclim.2022.831587

Garcia, M. O. (1996). Petrography and olivine and glass chemistry of lavas from the Hawaii Scientific Drilling Project. *J. Geophys. Res. Solid Earth* 101 (B5), 11701–11713. doi:10.1029/95jb03846

Gorring, M. L., and Naslund, H. (1995). Geochemical reversals within the lower 100 m of the Palisades sill, New Jersey. *Contributions Mineralogy Petrology* 119 (2-3), 263–276. doi:10.1007/bf00307286

Gulick, A. (1955). Phosphorus as a factor in the origin of life. *Am. Sci.* 43 (3), 479–489.

Haas, S., Sinclair, K. P., and Catling, D. C. (2024). Biogeochemical explanations for the world's most phosphate-rich lake, an origin-of-life analog. *Commun. Earth & Environ.* 5 (1), 28. doi:10.1038/s43247-023-01192-8

Hamilton, V. E., and Christensen, P. R. (2005). Evidence for extensive, olivine-rich bedrock on Mars. *Geology* 33 (6), 433–436. doi:10.1130/g21258.1

Hao, J., Glein, C. R., Huang, F., Yee, N., Catling, D. C., Postberg, F., et al. (2022). Abundant phosphorus expected for possible life in Enceladus's ocean. *Proc. Natl. Acad. Sci.* 119 (39), e2201388119. doi:10.1073/pnas.2201388119

Hausrath, E., and Brantley, S. (2010). Basalt and olivine dissolution under cold, salty, and acidic conditions: what can we learn about recent aqueous weathering on Mars? *J. Geophys. Res. Planets* 115 (E12). doi:10.1029/2010je003610

Herschy, B., Chang, S. J., Blake, R., Lepland, A., Abbott-Lyon, H., Sampson, J., et al. (2018). Archean phosphorus liberation induced by iron redox geochemistry. *Nat. Commun.* 9 (1), 1346. doi:10.1038/s41467-018-03835-3

Hsu, H.-W., Postberg, F., Sekine, Y., Shibuya, T., Kempf, S., Horányi, M., et al. (2015). Ongoing hydrothermal activities within Enceladus. *Nature* 519 (7542), 207–210. doi:10.1038/nature14262

Jahnke, R. A. (1992). "14 the phosphorus cycle," in *International geophysics* (Elsevier), 50, 301–315. doi:10.1016/s0074-6142(08)62697-2

Jan, M. Q., Khan, M. A., and Qazi, M. S. (1993). The Sapat mafic-ultramafic complex, Kohistan arc, north Pakistan. *Geol. Soc. Lond. Spec. Publ.* 74 (1), 113–121. doi:10.1144/gsl.sp.1993.074.01.09

Jusino-Maldonado, M., Rianço-Silva, R., Mondal, J. A., Pasek, M., Laneuville, M., and Cleaves, H. J. (2022). A global network model of abiotic phosphorus cycling on Earth through time. *Sci. Rep.* 12 (1), 9348. doi:10.1038/s41598-022-12994-9

Korsch, R., Kositcin, N., and Champion, D. (2011). Australian island arcs through time: geodynamic implications for the Archean and Proterozoic. *Gondwana Res.* 19 (3), 716–734. doi:10.1016/j.gr.2010.11.018

Lago, J. Revisiting Darwin's little pond as a method to liberate phosphorus from apatite under prebiotic hadean earth conditions. (2021).

Langmuir, C. H., and Broecker, W. (2012). *How to build a habitable planet: the story of earth from the big bang to humankind-revised and expanded edition.* Princeton University Press.

Li, Y., Zhang, A.-C., Chen, J.-N., Gu, L.-X., and Wang, R.-C. (2017). Formation of phosphorus-rich olivine in Dar al Gani 978 carbonaceous chondrite through fluid-assisted metamorphism. *Am. Mineralogist* 102 (1), 98–107. doi:10.2138/am-2017-5881

Liu, Y., Tice, M., Schmidt, M., Treiman, A., Kizovski, T., Hurowitz, J., et al. (2022). An olivine cumulate outcrop on the floor of Jezero crater, Mars. *Science* 377 (6614), 1513–1519. doi:10.1126/science.abo2756

Lohrmann, R., and Orgel, L. (1968). Prebiotic synthesis: phosphorylation in aqueous solution. *Science* 161 (3836), 64–66. doi:10.1126/science.161.3836.64

Lynn, K. J., Garcia, M. O., and Shea, T. (2020). Phosphorus coupling obfuscates lithium Geospeedometry in olivine. *Front. Earth Sci.* 8, 525919. doi:10.3389/feart.2020.00135

Lynn, K. J., Shea, T., and Garcia, M. O. (2017). Nickel variability in Hawaiian olivine: evaluating the relative contributions from mantle and crustal processes. *Am. Mineralogist* 102 (3), 507–518. doi:10.2138/am-2017-5763

Maciá, E., Hernández, M., and Oró, J. (1997). Primary sources of phosphorus and phosphates in chemical evolution. *Orig. Life Evol. Biosphere* 27, 459–480. doi:10.1023/A:1006523226472

Mason, B. (1981). ALHA77005 petrographic description. *Antarct. Meteor. Newsl.* 4, 12.

McKibbin, S. J., Pittarello, L., Makarona, C., Hamann, C., Hecht, L., Chernonozhkin, S. M., et al. (2019). Petrogenesis of main group pallasite meteorites based on relationships among texture, mineralogy, and geochemistry. *Meteorit. & Planet. Sci.* 54 (11), 2814–2844. doi:10.1111/maps.13392

McSween, H. Y., Wyatt, M. B., Gellert, R., Bell, I. I. I. J. F., Morris, R. V., Herkenhoff, K. E., et al. (2006). Characterization and petrologic interpretation of olivine rich basalts at Gusev Crater, Mars. *J. Geophys. Res. Planets* 111 (E2). doi:10.1029/2005je002477

Milman-Barris, M. S., Beckett, J. R., Baker, M. B., Hofmann, A. E., Morgan, Z., Crowley, M. R., et al. (2008). Zoning of phosphorus in igneous olivine. *Contributions Mineralogy Petrology* 155, 739–765. doi:10.1007/s00410-007-0268-7

Mustard, J., Poulet, F., Gendrin, A., Bibring, J.-P., Langevin, Y., Gondet, B., et al. (2005). Olivine and pyroxene diversity in the crust of Mars. *Science* 307 (5715), 1594–1597. doi:10.1126/science.1109098

Mysen, B. (1996). Phosphorus speciation changes across the glass transition in highly polymerized alkali silicate glasses and melts. *Am. Mineralogist* 81 (11-12), 1531–1534. doi:10.2138/am-1996-11-1226

Mysen, B. O. (2011). Amorphous Materials: an experimental study of phosphorous and aluminosilicate speciation in and partitioning between aqueous fluids and silicate melts determined *in-situ* at high temperature and pressure. *Am. Mineralogist* 96 (10), 1636–1649. doi:10.2138/am.2011.3728

Olsen, A. A., Hausrath, E. M., and Rimstidt, J. D. (2015). Forsterite dissolution rates in Mg sulfate rich Mars analog brines and implications of the aqueous history of Mars. *J. Geophys. Res. Planets* 120 (3), 388–400. doi:10.1002/2014je004664

Osland, R. (1997). *Modelling of variations in Norwegian olivine deposits. Doktor Ingeniør Thesis.* Trondheim, Norway: Norwegian Univ of Science and Technology.

Pappalardo, R. T., Belton, M. J., Breneman, H., Carr, M., Chapman, C. R., Collins, G., et al. (1999). Does Europa have a subsurface ocean? Evaluation of the geological evidence. *J. Geophys. Res. Planets.* 104 (E10), 24015–24055. doi:10.1029/1998je000628

Pasek, M., and Block, K. (2009). Lightning-induced reduction of phosphorus oxidation state. *Nat. Geosci.* 2 (8), 553–556. doi:10.1038/ngeo580

Pasek, M. A. (2008). Rethinking early Earth phosphorus geochemistry. *Proc. Natl. Acad. Sci.* 105 (3), 853–858. doi:10.1073/pnas.0708205105

Pasek, M. A., Dworkin, J. P., and Lauretta, D. S. (2007). A radical pathway for organic phosphorylation during schreibersite corrosion with implications for the origin of life. *Geochimica Cosmochimica Acta* 71 (7), 1721–1736. doi:10.1016/j.gca.2006.12.018

Pasek, M. A., Omran, A., Feng, T., Gull, M., Lang, C., Abbatiello, J., et al. (2022). Serpentinization as a route to liberating phosphorus on habitable worlds. *Geochimica Cosmochimica Acta* 336, 332–340. doi:10.1016/j.gca.2022.09.027

Paytan, A., and McLaughlin, K. (2007). The oceanic phosphorus cycle. *Chem. Rev.* 107 (2), 563–576. doi:10.1021/cr0503613

Pokrovsky, O. S., and Schott, J. (2000). Kinetics and mechanism of forsterite dissolution at 25°C and pH from 1 to 12. *Geochimica Cosmochimica Acta* 64 (19), 3313–3325. doi:10.1016/s0016-7037(00)00434-8

Postberg, F., Sekine, Y., Klenner, F., Glein, C. R., Zou, Z., Abel, B., et al. (2023). Detection of phosphates originating from Enceladus's ocean. *Nature* 618 (7965), 489–493. doi:10.1038/s41586-023-05987-9

Reimann, R., and Zubay, G. (1999). Nucleoside phosphorylation: a feasible step in the prebiotic pathway to RNA. *Orig. Life Evol. Biosphere* 29, 229–247. doi:10.1023/a:1006580009791

Renna, M. R., and Tribuzio, R. (2011). Olivine-rich troctolites from Ligurian ophiolites (Italy): evidence for impregnation of replacive mantle conduits by MORB-type melts. *J. Petrology* 52 (9), 1763–1790. doi:10.1093/petrology/egr029

Roberge, J., Delgado-Granados, H., Wallace, P., and Kent, A. (2007). *Pre-eruptive volatile contents of mafic magma at Popocatepetl volcano, Mexico, from olivine-hosted melt inclusions* (San Francisco, California: AGU Fall Meeting Abstracts).

Roberts, J. H., and Nimmo, F. (2008). Tidal heating and the long-term stability of a subsurface ocean on Enceladus. *Icarus* 194 (2), 675–689. doi:10.1016/j.icarus.2007.11.010

Schoffstall, A. M. (1976). Prebiotic phosphorylation of nucleosides in formamide. *Orig. life* 7 (4), 399–412. doi:10.1007/bf00927935

Schubert, G., Sohl, F., and Hussmann, H. (2009). "Interior of europa," in *Europa*, Editors R. T. Pappalardo, W. B. McKinnon, and K. Khurana (Tucson, AZ: University of Arizona press), 353–367.

Segami, S., Asaoka, M., Kinoshita, S., Fukuda, M., Nakanishi, Y., and Maeshima, M. (2018). Biochemical, structural and physiological characteristics of vacuolar H+-pyrophosphatase. *Plant Cell Physiology* 59 (7), 1300–1308. doi:10.1093/pcp/pcy054

Shea, T., Hammer, J. E., Hellebrand, E., Mourey, A. J., Costa, F., First, E. C., et al. (2019). Phosphorus and aluminum zoning in olivine: contrasting behavior of two nominally incompatible trace elements. *Contributions Mineralogy Petrology* 174, 85–24. doi:10.1007/s00410-019-1618-y

Shea, T., Lynn, K. J., and Garcia, M. O. (2015). Cracking the olivine zoning code: distinguishing between crystal growth and diffusion. *Geology* 43 (10), 935–938. doi:10.1130/g37082.1

Thomas, P., Tajeddine, R., Tiscareno, M., Burns, J., Joseph, J., Loredo, T., et al. (2016). Enceladus's measured physical libration requires a global subsurface ocean. *Icarus* 264, 37–47. doi:10.1016/j.icarus.2015.08.037

Trommsdorff, V., Sánchez-Vizcaíno, V. L., Gómez-Pugnaire, M., and Müntener, O. (1998). High pressure breakdown of antigorite to spinifex-textured olivine and orthopyroxene, SE Spain. *Contributions Mineralogy Petrology* 132, 139–148. doi:10.1007/s004100050412

Turner, B. L., Mahieu, N., and Condron, L. M. (2003). The phosphorus composition of temperate pasture soils determined by NaOH–EDTA extraction and solution 31P NMR spectroscopy. *Org. Geochem.* 34 (8), 1199–1210. doi:10.1016/s0146-6380(03)00061-5

Tyrrell, T. (1999). The relative influences of nitrogen and phosphorus on oceanic primary production. *Nature* 400 (6744), 525–531. doi:10.1038/22941

Walton, C. Phosphorus pathways in deep time 2022.

Walton, C. R., Baziotis, I., Cernok, A., Ferrière, L., Asimow, P. D., Shorttle, O., et al. (2021b). Microtextures in the Chelyabinsk impact breccia reveal the history of Phosphorus Olivine Assemblages in chondrites. *Meteorit. & Planet. Sci.* 56 (4), 742–766. doi:10.1111/maps.13648

Walton, C. R., Shorttle, O., Jenner, F. E., Williams, H. M., Golden, J., Morrison, S. M., et al. (2021a). Phosphorus mineral evolution and prebiotic chemistry: from minerals to microbes. *Earth-Science Rev.* 221, 103806. doi:10.1016/j.earscirev.2021.103806

Welsch, B., Faure, F., Famin, V., Baronnet, A., and Bachèlery, P. (2013). Dendritic crystallization: a single process for all the textures of olivine in basalts? *J. Petrology* 54 (3), 539–574. doi:10.1093/petrology/egs077

Welsch, B., Hammer, J., and Hellebrand, E. (2014). Phosphorus zoning reveals dendritic architecture of olivine. *Geology* 42 (10), 867–870. doi:10.1130/g35691.1

Westall, F., Hickman-Lewis, K., Hinman, N., Gautret, P., Campbell, K. A., Bréhéret, J.-G., et al. (2018). A hydrothermal-sedimentary context for the origin of life. *Astrobiology* 18 (3), 259–293. doi:10.1089/ast.2017.1680

Xu, J., Green, N. J., Gibard, C., Krishnamurthy, R., and Sutherland, J. D. (2019). Prebiotic phosphorylation of 2-thiouridine provides either nucleotides or DNA building blocks via photoreduction. *Nat. Chem.* 11 (5), 457–462. doi:10.1038/s41557-019-0225-x